IMPLEMENTATION OF A LONG PATH MULTI-REFLECTION OPTICAL CELL

WITH A MID-INFRARED FREQUENCY COMB LASER SOURCE FOR SENSITIVE

MOLECULAR SPECTROSCOPY

A Thesis

by

RUQAYYAH F. M. H. H. ASKAR

Submitted to the Office of Graduate and Professional Studies of
Texas A&M University
in partial fulfillment of the requirements for the degree of

MASTER OF SCIENCE

Chair of Committee,	Hans A. Schuessler
Committee Members,	Dong Hee Son
	M. Suhail Zubairy
Head of Department,	George R. Welch

May 2014

Major Subject: Physics

ABSTRACT

Multi-reflection optical cells are used in a wide variety of applications. They are commonly used as optical pumping systems and as optical delay lines. One of the most important applications of multi-reflection optical cells is in the field of gas detection and gas concentration measurements. This includes applications in industry and in global warming studies. The global concern regarding greenhouse trace gases is increasing with the ongoing industrial growth and the upraising needs of the total population on Earth nowadays, in addition to the big influence on the global climate stability. This resulted in an accelerated development of trace gas detection techniques in many fields over the last years. Molecular spectroscopy is one of the most powerful techniques available today. It provides highly sensitive and selective measurements of greenhouse trace gases and their isotopic ratios not only for indoor samples but also for atmospheric estimations and in-situ measurements.

In this research, a long path multi-reflection optical cell is implemented in the first part for highly sensitive molecular spectroscopy applications. In the second part, two mid-infrared frequency combs are characterized by their experimentally revealed broad-band spectra and interferometric autocorrelation traces. The use of a long path multi-reflection cell along with a highly coherent characterized broad-band frequency comb laser source allows for sensitive molecular spectroscopic measurements over a broad bandwidth for the detection of various greenhouse gases on a short time scale. In the mid-infrared region, also known as infrared fingerprint region, methane and almost all the molecules have sharp

rotational-vibrational absorption intensities, which brought a noticeable interest to the mid-infrared region for trace gas detection experiments. Based on this, preliminary results of dual frequency comb molecular absorption spectroscopy, as the third and the final part of this experiment, are presented as an application of the long optical path multi-reflection cell based on mid-infrared frequency comb laser sources centered at 3.2 μm for the detection of methane in ambient air. A concentration of 1.2 ppmv is reported in this experiment for methane in our laboratory's environment where a relative humidity level of 4% produces a strong background of water lines.

ACKNOWLEDGEMENTS

Finally, my deepest thanks to my mother and father for raising me the way they did, and for their encouragement and continuous support, and to my husband for his patience and love.

TABLE OF CONTENTS

LIST OF FIGURES

CHAPTER I

INTRODUCTION

1.1 Trace Gas Detection

The need has risen in the last decades for accurate regular monitoring of the atmospheric climate changes due to global warming and their consequent effects on life in different environments. A crucial step towards a future where global warming is controlled is to have a real time sensitive measurements and a reliable long term observations about the current concentrations and isotopic ratios of greenhouse trace gases. This is one of the main motives behind the ongoing development of different detection techniques and procedures in various fields of science: physics, engineering, chemistry, and biosciences.

1.2 Molecular Absorption Spectroscopy Techniques

Molecular absorption spectroscopy is one of the driving fields in trace gas detection. It can be performed on gas samples indoors by means of an optical cavity and a gas chamber, or outdoors for direct sensitive in-situ measurements. Wavelength-modulation technique (WMS), Faraday-rotation spectroscopy (FRS), and Fourier transform spectroscopy are examples of techniques used in the molecular spectroscopy research area [1].

Other examples involving molecular absorption spectroscopy are cavity ring-down spectroscopy (CRDS), off-axis integrated cavity output spectroscopy (OA-ICOS),

and incoherent broad-band cavity enhanced absorption spectroscopy (IBBCEAS). The last three are often categorized under the term cavity-enhanced absorption spectroscopy (CEAS) [1, 2]. Dual comb Fourier transform spectroscopy is another example that has emerged in the last years as a new technique for precision molecular spectroscopy. Using one of these techniques along with a modern probe light source and a low-noise detector can provide high-sensitivity measurements for detection of different trace gas molecules.

Carbon dioxide and methane in particular, as the first and second gas molecules responsible for global warming respectively, have been widely investigated by scientists around the world. An isotopic ratio measurement of CH_4 in ambient air is reported by H. Dahnke and co-workers [3]. In this work they have used a mid-infrared laser source based on cavity ring-down technique. Thorpe and Ye used different detection schemes in detection of CO_2, C_2H_2, NH_3, and CO based on cavity-enhanced direct frequency comb spectroscopy [4]. Zhu et al studied the absorption spectrum of C_2H_2 in the near infrared with real-time dual frequency comb spectroscopy [5]. A detection limit of 130 ppb for H_2O_2 in the presence of 3% of water was reported by Foltynowicz et al by cavity-enhanced frequency comb Fourier transform absorption spectroscopy at 3.9 μm [6].

1.3 Long Effective Path Length

Multi-reflection optical cells are often used in absorption spectroscopy experiments to allow for a longer path length through the sample. According to the Beer-Lambert law, equation (1), under the same concentration, the longer the path length is,

the more molecules contribute to the absorption signal resulting in more sensitive absorption measurements.

$$\frac{I}{I_o} = e^{-\alpha L}$$ (1)

Here, I_o is the intensity of the incident light beam, I is the intensity of the transmitted light beam, L is the absorption path length, and α is the absorbance. It is also referred to as the absorption coefficient, and it can be written as $\alpha = N\sigma$, with N being the number density of the absorbing molecules and σ being the cross-section of light absorption by each molecule.

Spectroscopic experiments that use multi-reflection optical cells usually require a small aperture on a mirror in one side of the cavity. One aperture is used, in some cases, as the entrance and exit aperture. In other cases two apertures are required, one to enter and one to exit the multi-reflection cell.

When the experiment is taking place, the light beam enters the optical cell from the entrance aperture, gets reflected multiple times, then exits via the exit aperture. When the light is getting reflected and bouncing between the two cavity-mirrors, it is exposed to a wanted absorption, but it also suffers from unwanted optical losses due to the diffraction of light. In addition, the reflectivity of the mirrors is a limiting factor that must be considered in multi-reflection cells' designs. Therefore, a good mode-matching and the use of highly reflective mirrors are essential.

Another major point in multi-reflection cells is the path length during which the light-matter interaction occurs. Thus, designing long cavities and considering the maximum possible number of reflections is crucial in experiments with multi-reflection

3

cells. Claude Robert investigated atmospheric CO and CO_2 in the near infrared using a multiple-reflection optical cell of 130 reflections and 140.3 m optical path length. The mirrors Robert used have protective gold coating with 98% reflectivity [7]. A 3σ MDC of 300 pptv was reported for HONO by Lee et al for a 1-s integration time using a multi-reflection cell with 210 m absorption path length [8].

1.4 Detection Schemes

The first detection scheme that comes to the mind in experiments which involve observing an optical spectrum is the use of an optical monochromator. It is simple to use, since it only requires sending the output of a light source and focusing it into the entrance slit of the monochromator, and then starting the mechanical wavelength scanning. However, it also requires high-enough output power since after diffraction the total output power spreads over all spectral lines. In such a case, a sensitive detector is required with appropriate response limits.

In cases where the output power is low or not high enough for the available detector to respond, Fourier transform spectroscopy is the alternative detection technique. It mainly includes a beam splitter and two mirrors; one is fixed in position and the other moves with a known speed. At an intermediate position of the moving mirror, the two arms of the spectrometer match in length which results in total overlapping and thus a sharp burst at the center of an interferogram in the time domain. After the Fourier transform of the interferogram, it reveals the desired optical spectrum in the frequency domain.

A novel detection scheme that is sensitive and powerful in precision molecular spectroscopy is dual comb spectroscopy. This type of Fourier transform spectroscopy uses two mode-locked frequency comb laser sources with a slightly different repeating rates. The first one is responsible of exciting the free induction decay (FID) of the trace gas molecule in the beam path, while the second serves to interfere with the train of pulses of the first source. This produces an interferogram in the time domain. In the frequency domain, the Fourier transform of the interferogram is in the radio frequency region so it can be observed with a single detector, which in turn is connected to a sampling oscilloscope. Calibrating the data then reveals the absorption spectrum of the gas molecule under study.

1.5 Dual Comb Fourier Transform Spectroscopy

This section describes the dual comb spectroscopy in more detail. Fig. 1 shows a picture of the time and frequency domains of Fourier transform spectroscopy [5, 9]. In general, the optical frequency comb structure is described using $f_n = nf_r + f_o$ where f_n is the laser frequency, f_r is the repetition rate of the frequency comb, and f_o is the carrier-envelop offset frequency [10, 11]. In dual comb spectroscopy, two optical frequency combs of very close repetition rates are used. In the time domain, the two trains of pulses interfere to generate a cross-correlation interferogram I(t). A free induction decay (FID) signal, resulting from rotational-vibrational transitions of the molecules present in the gas sample, will be produced after the comb passes through the sample. The middle pulse of source1, in Fig. 1 (a), fully overlaps with the middle pulse of source2 giving the sharpest

peak, which is usually refers to as the center burst [5, 9]. The second two pulses around the middle one are shifted by the difference in the repetition rates Δf_r (denoted in Fig. 1 by δ), resulting in a partial overlapping of the pulses and their corresponding FID signal, and so on. In the frequency domain, shown in Fig. 1 (b), the comb lines of the two sources are combined converting the resulting spectrum to frequencies that can be detected and analyzed with the available signal processing devices. The conversion follows the relation $\Delta f_o + n \, \Delta f_r$ where Δf_o is the difference between the carrier-envelope offset frequencies, Δf_r is the difference between the repetition rates, and n is an integer.
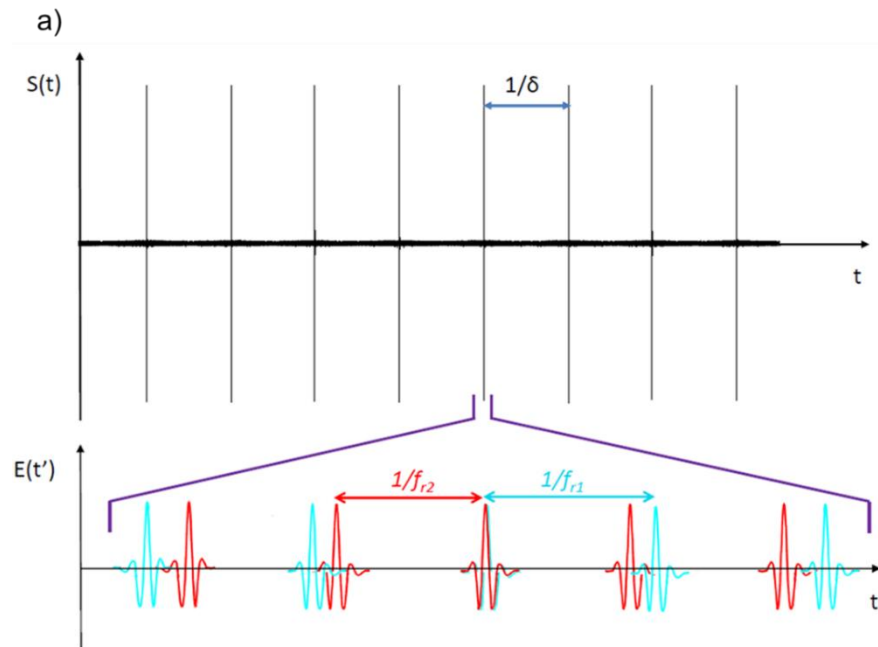
Fig. 1: (a) Time-domain and (b) frequency-domain pictures of dual comb Fourier transform spectroscopy

b)

Fig. 1: Continued

7
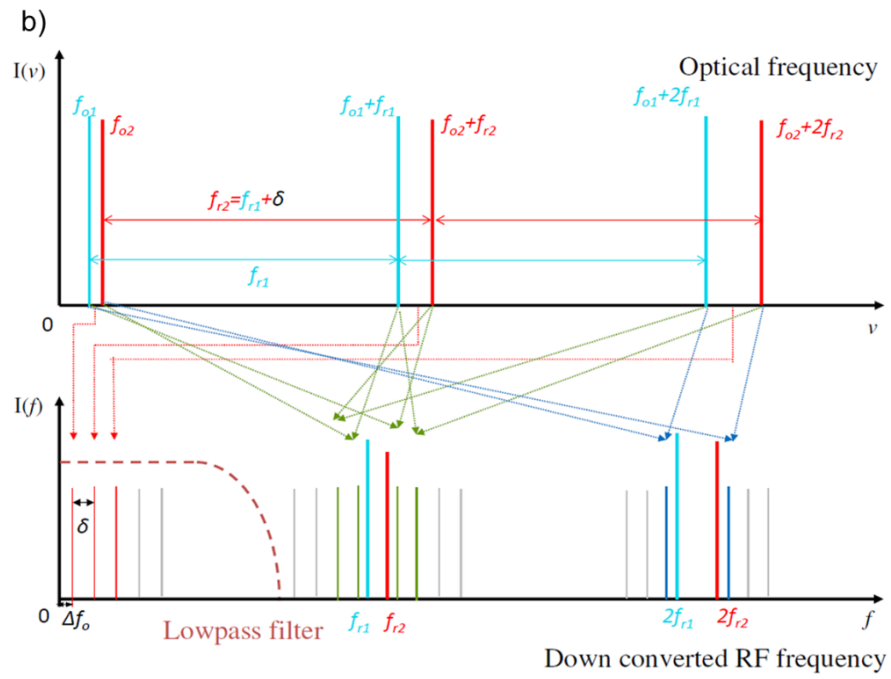
CHAPTER II

LONG PATH MULTI-REFLECTION OPTICAL CELL

2.1 Description

The design of the multi-reflection optical cell implemented in this experiment was first proposed by Shouhua Chen as a part of his master degree thesis. He used a computer program to maximize and depict the spots pattern and count the number of reflections between the optical cell mirrors before the beam exits the cell from the same entrance aperture.

The multi-reflection optical cell conceptually consists of four square mirrors fixed at each end of an optical cavity, with only one aperture on one of the eight cavity mirrors. The four mirrors at each end can be considered as one mirror, and are adjustable so that the beam can be redirected to have the spots overlap after multiple reflections. The mirrors are rigidly mounted at the two ends of 1 m long glass vacuum chamber.

When the environmental conditions change, the multi-reflection cell might become misaligned or, at minimum, out of overlapping. Therefore, it is necessary before taking any measurements to adjust the mirrors until the desired spot pattern and the maximum output power are obtained. The spots where the beam hits the mirrors' surfaces are determined with the help of the computer program written by Shouhua Chen. The program also estimates the number of reflections inside the optical cell before the beam exits from the same entrance aperture, and by that it estimates the path the beam travels. For the multi-reflection cell in this experiment, the number of reflections is 579, and the

length of the optical cavity is 1 m, which gives a total absorption path length of 580 m. This long interaction path length between the laser beam and the gas sample inside the multi-reflection cell opens the door for sensitive molecular absorption measurements.

2.2 Implementation and Alignment

Six mirrors of 1 m radius of curvature are used instead of eight mirrors. Three are place at each of the two ends of the long glass call, as shown in Fig. 2. The bottom mirrors at both sides, in the original proposed design, are merged into one in order to reduce the alignment difficulty. In other words, a rectangular mirror is used instead of two square mirrors at the bottom of each side. The mirror with the entrance-exit aperture is on the top right at one side of the cell. Each mirror can be adjusted horizontally and vertically and tilted in 3-dimentions to have its center and its tilting angle as evaluated by the previously mentioned computer program.
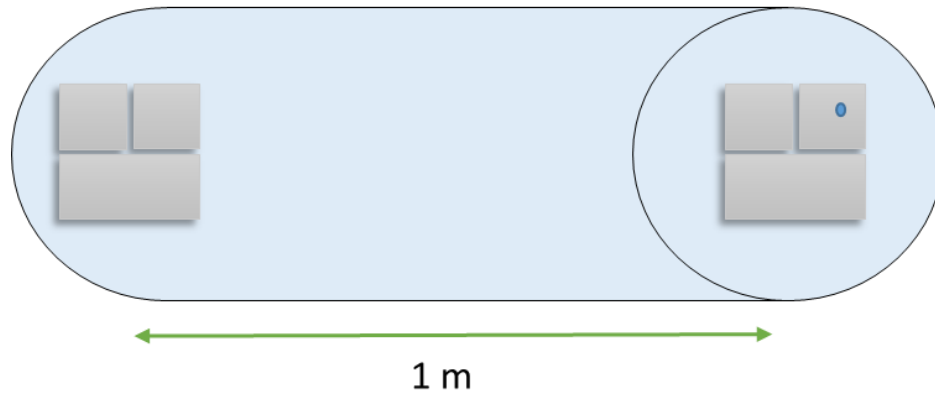
Fig. 2: The design of the multi-reflection optical cell

The light source used in this experiment is a mid-infrared laser source, which will be discussed in next chapters. As the infrared light is invisible to the human eye, a visible laser beam has been commonly used in infrared laser spectroscopy for alignment purposes. This experiment uses a red alignment laser since the mirrors here have high reflectivity in the red light region as well. The wavelength of this red laser is around 685 nm and can change slightly with a change in the temperature or the driving current.

The beam from the red alignment laser is redirected by two alignment mirrors into the multi-reflection cell through the entrance aperture. The spot pattern, shown in Fig. 3, is followed as a reference to adjust the horizontal and vertical positions of the mirrors one by one. In more detail, when the beam first enters the multi-reflection cell, through the aperture labeled by the number 1, it is aligned by the two alignment mirrors to hit on spot 1' as Fig. 3 shows. Then the mirror which has the spot 1' is adjusted, vertically or

horizontally or both, to have the beam hitting spot 2. This procedure of following the pattern, by the numbers and their images, and adjusting the mirrors goes on until all mirrors are adjusted and an exit beam is detected. This tells that the beam has successfully been reflected many times and followed the same path out of the multi-reflection optical cell, as required. After this, the procedure continues with alternating fine tuning until the maximum output power is obtained.

After having the multi-reflection cell well-aligned, two apertures are used to mark this optimum injection direction. These two marking apertures not only help to easily get the spot pattern back if it gets misaligned, but also are used to easily inject the infrared laser beam along the same beam path of the alignment laser.

12'	14'	16'	18'	20'	22'	24'
10'						26'
8'						1'
6'						3'
4'						5'
2'						7'
27'						9'
23'/25'	21'	19'	17'	15'	13'	11'

5	7	9	11	13	15	17	
3	30					19	
(1)	28					21	
	26					23	
	24					25	
	22					27	
	20					29	2
	18	16	14	12	10	8	4/6
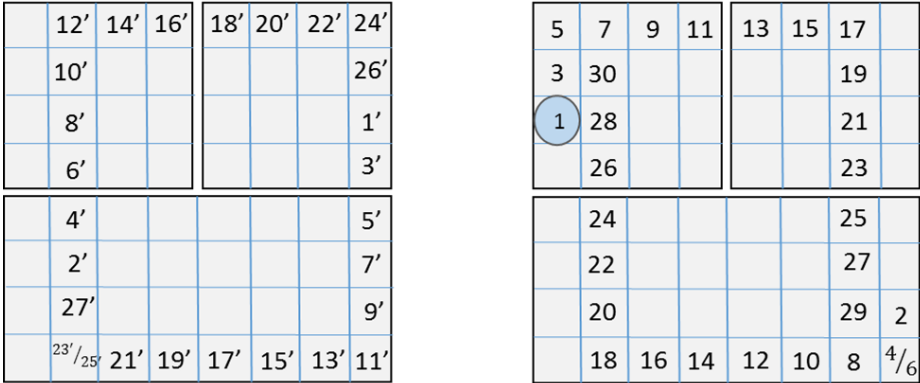
Fig. 3: The first-spots pattern

The maximum recorded power out of the multi-reflection cell for the alignment laser is about 4 mW, with a good spatial overlapping of the spots, as shown in Fig. 4.

When the outside temperature changes, a reduction in the output power is noticed. This is due to the effect of the temperature change on drifting the beam or on tilting the mirrors slightly, which misaligns the overlapping of the spots. The humidity level is another concern since a high humidity level causes more water vapor absorption to take place which results in a low output power form the multi-reflection optical cell.
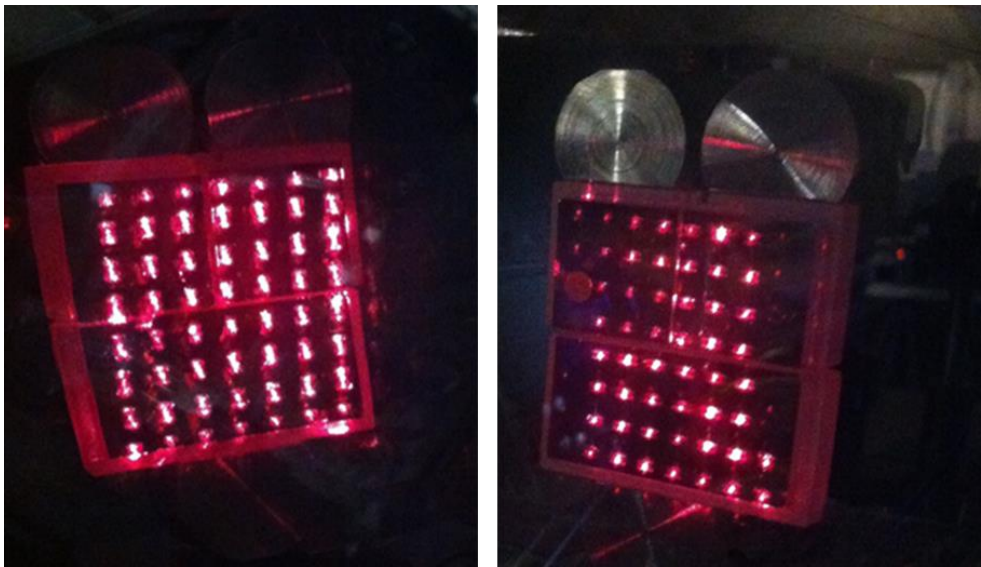
Fig. 4: The experimental spots pattern using the red alignment laser

CHAPTER III

CHARACTERIZATION OF FREQUENCY COMBS

3.1 Spectra of the Two Frequency Combs

A 0.3 m McPherson scanning monochromator, shown in the setup of Fig. 5, is used for finding the broadband spectra generated by the two laser sources one at a time. The beam from the laser source is sent to two alignment mirrors, to align its propagation direction toward the entrance slit of the monochromator, and then to a focusing lens to focus it on the entrance slit of the monochromator.

As the beam enters the monochromator and reflects on the first mirror, it gets collimated by this mirror and redirected into a diffraction grating. Then it diffracts from the groves on the surface of the grating and travels to the center of the second mirror, the focusing mirror. The different components of the light source, due to the wavelength-dependent angles of the diffraction grating, spread over a linear spectrum at the other end of the monochromator. An exit slit at this end allows a single spectral component, or a narrow section of the spectrum, to pass into the detector.

The size of the slit can be changed, from 2mm to 5 µm, to enhance the resolution and have a narrower section of the optical spectrum passing through. The diffraction grating can be rotated to choose the portion of the spectrum to be investigated, either manually by hand or mechanically by setting the monochromator to scan the spectrum between two specific wavelengths. In this experiment, the monochromator scans mechanically from low to high wavelength ranges (2.8 µm to 3.8 µm).

13
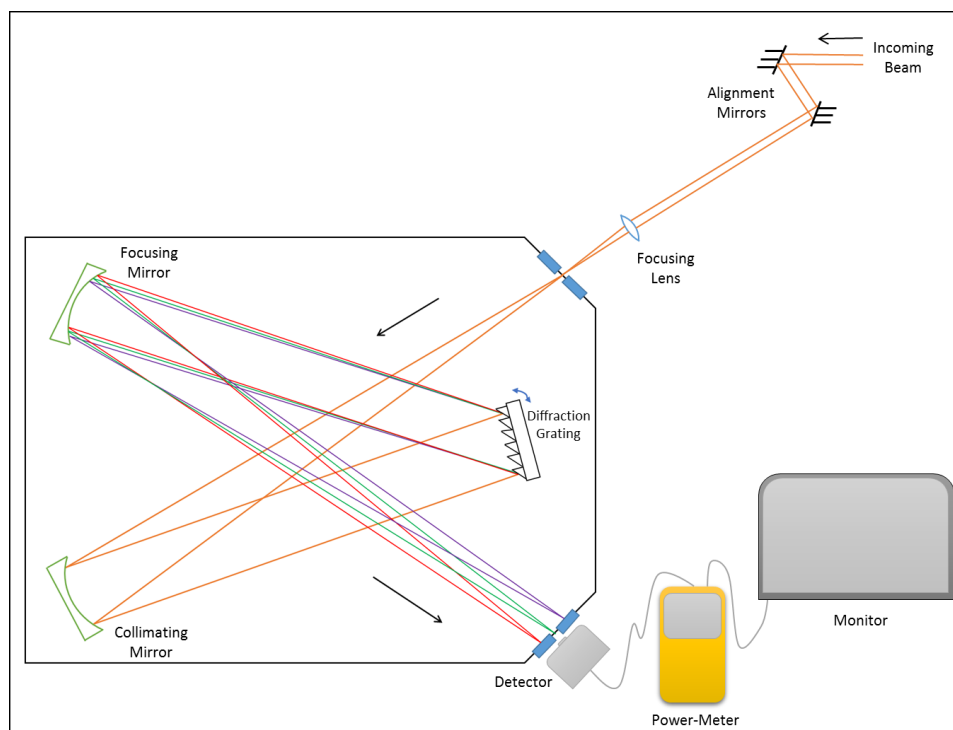
Fig. 5: Schematic of the monochromator experimental setup

A power meter is used to detect the light coming out of the exit slit, and is placed right after the exit slit. The reading on the power-meter is recorded on a computer using a software that comes along with the power-meter. The experimental setup is shown in Fig. 5. In order to read the whole spectrum, the mechanical scan switch in the monochromator is turned on and the scanning direction is chosen either to be from low wavelength range to high wavelength range or vice versa. Over all, the monochromator scans the whole desired region of the spectrum, and the thermal detector detects and sends the reading at each wavelength to the computer to record it and thus records the final spectrum.

The monochromator has ten different scanning speeds from which a speed of 500 A°/min was chosen to scan with. One of the reasons behind a low resolution spectrum is the limited response of the detector to the changes in the signal. The scanning speed can be changed from 500 A°/min to 1000 A°/min to match the low response of the detector, but this will also reduce the resolution of the spectrum which takes us away from the goal here.

The spectra of the two mid-infrared frequency comb laser sources used in this experiment are recorded following the procedure described above. Fig. 6 and Fig. 7 shows the normalized power spectral density of the two sources, respectively. Using a slit size of 100 μm, $\lambda = 3.25$ μm, spectrum's length of 40 nm, and the bandwidth of the generated spectrum 800 nm, the spectral resolution is estimated to be around 60 GHz. This spectral resolution is calculated using the relation $\Delta f = \frac{c}{\lambda^2} \times \Delta\lambda$ where $\Delta\lambda = \frac{Slit\ size}{Length\ of\ spectrum} \times Bandwidth$ and c is the speed of light.
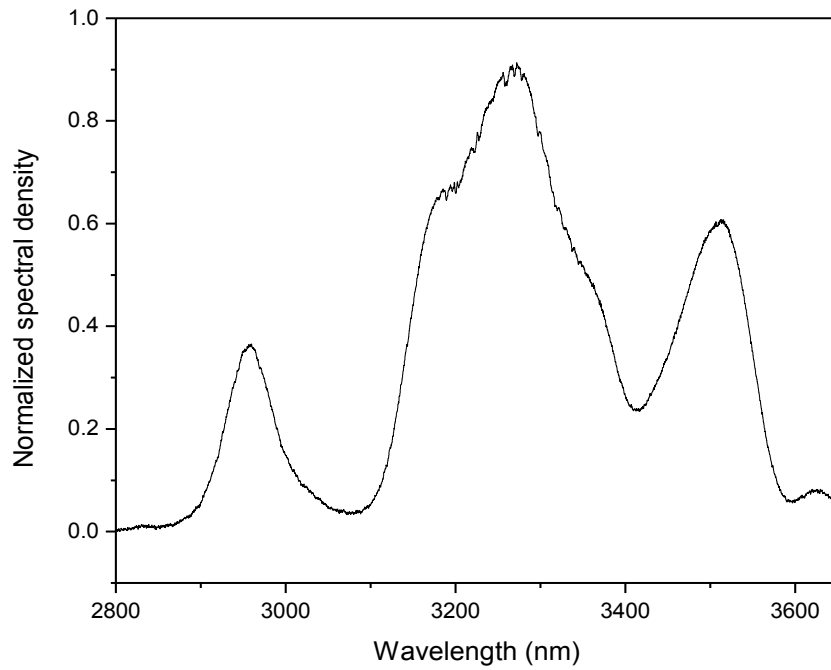
Fig. 6: The experimental spectrum of comb1
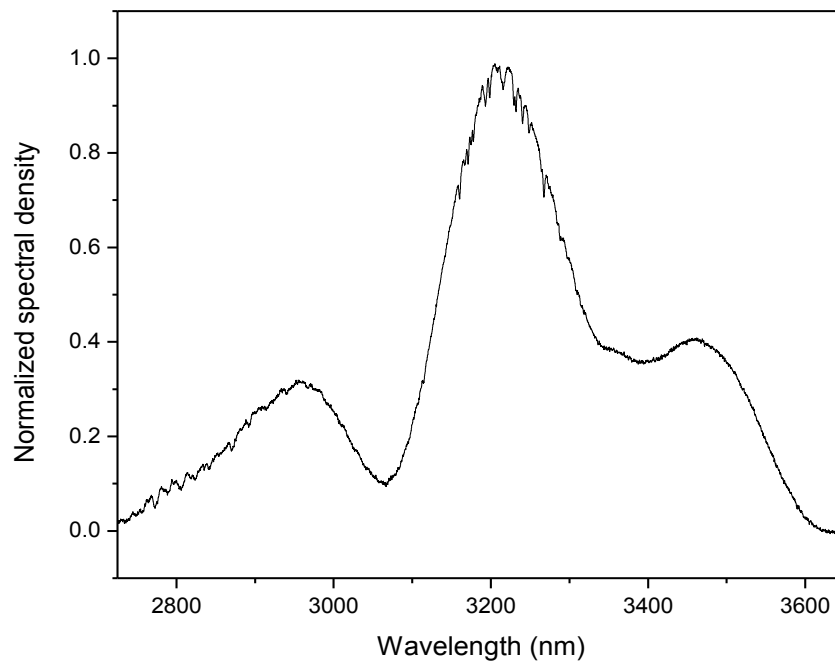

Fig. 7: The experimental spectrum of comb2

16

3.2 Interferometric Autocorrelation Traces

The beam coming from the laser source is directed to the interferometric autocorrelation experimental setup, illustrated in Fig. 8. With the help of two alignment mirrors, the beam passes through two pin-holes (apertures) into a beam splitter. The use of the pin-holes is necessary for alignment purposes since the mid-infrared light is invisible to the human eye. The light beam transmitted from the beam splitter reflects on a mirror fixed in position, so it covers twice the distance between the BS and the mirror. The reflected part form the beam splitter goes to a moving mirror then reflects back, also covering twice the distance. The speed of the translational stage that holds the second mirror is controlled by a connected movement controller. After the beams at the two arms are back at the BS they overlap, and a flipping mirror redirects them to a lens which focuses them to a photo-detector with a nonlinear effect. Either a nonlinear second harmonic generation crystal is used in autocorrelation setups, or a nonlinear two-photon absorption photodiode. The detector used in this interferometer is an InGaAs photodiode (Hamamatsu G8376-03) where two-photon absorption takes place.
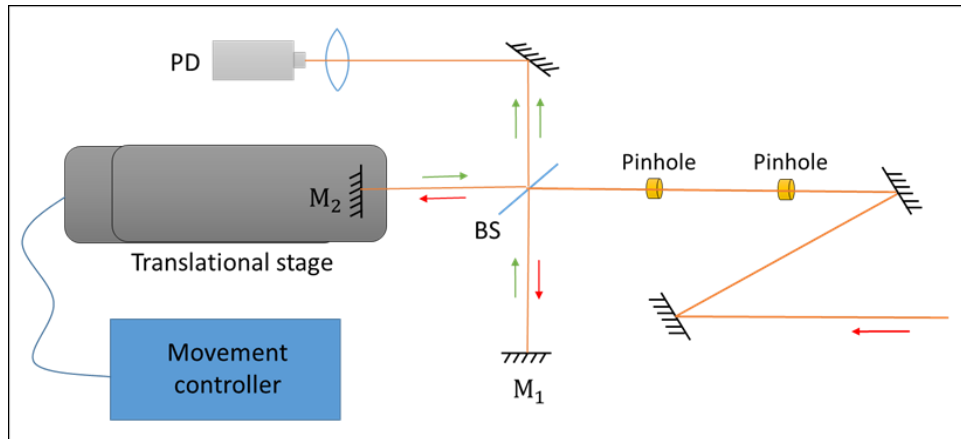
Fig. 8: Schematic of the interferometric autocorrelation setup

The maximum intensity is recorded by the detector when the two arms of the spectrometer are equal, which implies that the overlapping of the two pulses is maximum. With the movement of the stage, the beams at the two arms cover slightly different lengths, so the two beams overlap partially, and so on. The result is called interferometric autocorrelation trace, shown in Fig. 9 and Fig. 10 for the two comb sources, and is often used in temporal characterization purposes of laser sources. Assuming a Gaussian pulse shape, both interferometric autocorrelation traces correspond to a pulse duration of about 80 fs.
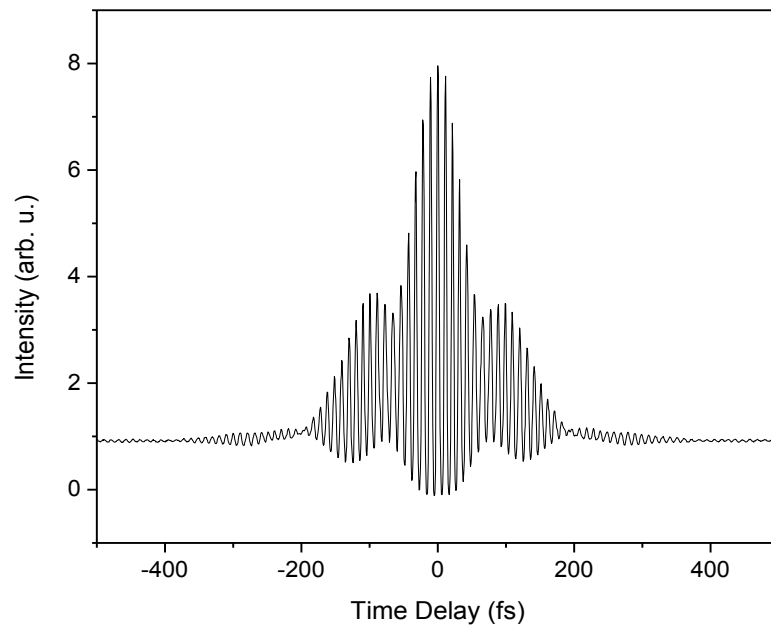
Fig. 9 : The experimental autocorrelation trace of frequency comb1
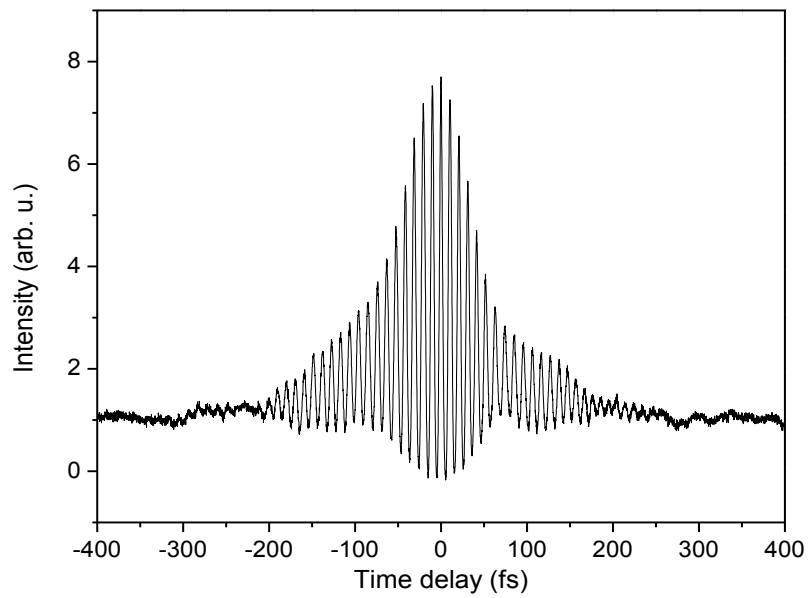
Fig. 10 : The experimental autocorrelation trace of frequency comb2

3.3 Comparison between the Two Frequency Combs

In dual frequency comb spectroscopic experiments, it is important to consider the overlapping of the spectra of the two comb sources. This step ensures taking the advantage of the highest possible spectral power at the spectral region of interest, which contributes significantly to the signal to noise ratio (SNR) of the spectroscopic measurements. Fig. 11 addresses the overlapping of the spectra of the two mid-infrared frequency comb laser sources used in this experiment.
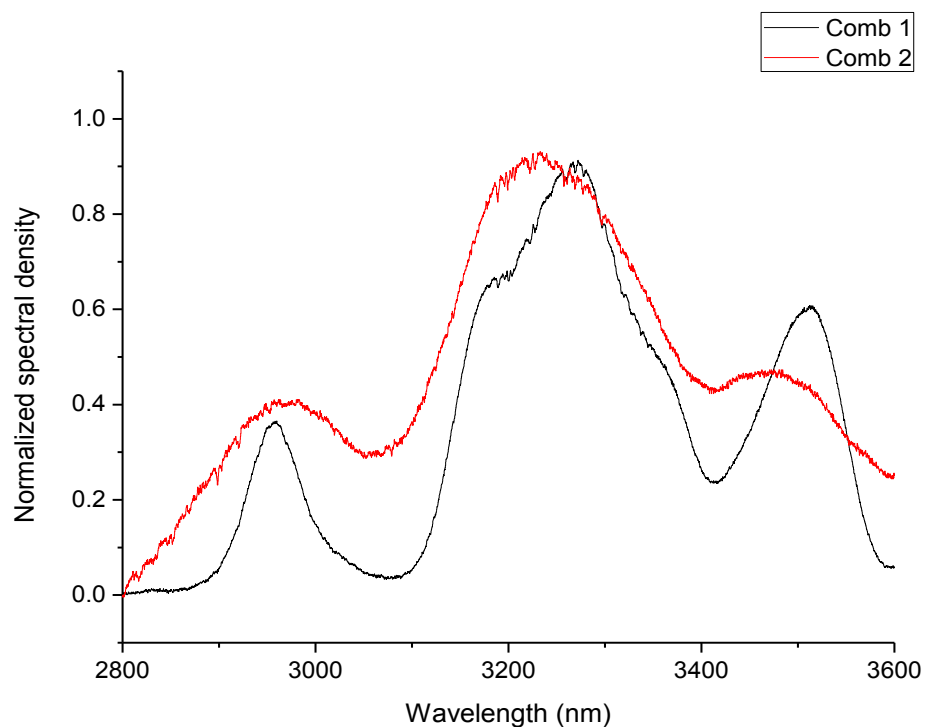
Fig. 11 : Overlapping of the spectra of the two mid-infrared frequency combs

CHAPTER IV

EXPERIMENT AND PRELIMINARY RESULTS

4.1 Characterizing the Gaussian Beam Profile

The Gaussian beam profile can be understood from Fig. 12. The beam waist at any point z along the axis of propagation can be found from equation (2) [12]:

$$w(z) = w_0 \sqrt{1 + \left(\frac{z}{z_R}\right)^2} \qquad\qquad (2)$$

where w_0 is the waist of the laser beam located at $z = 0$, and z_R is the Rayleigh range $z_R = \frac{\pi \, w_0{}^2}{\lambda}$ where $w(z_R) = w_0 \sqrt{2}$. The radius of curvature of the beam's wavefront at a distance z from its waist is expressed in this formula, equation (3) [12]:

$$R(z) = z \left(1 + \left(\frac{z}{z_R}\right)^2\right) \qquad\qquad (3)$$
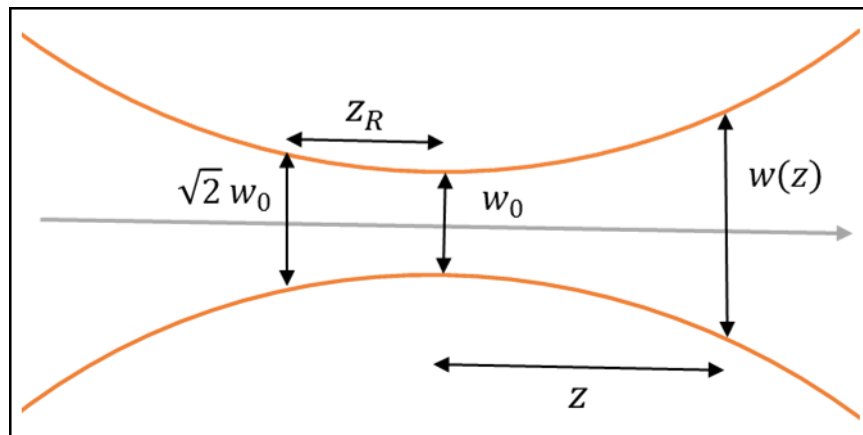
Fig. 12 : The Gaussian beam waist

A knife-edge method is used to find the beam width at a specific location. Solving the following integrals, (4) and (5), for the intensity of the Gaussian beam distribution with a normalization factor $C = \int_{-\infty}^{+\infty} e^{\frac{-2x^2}{w^2}} dx$, gives the percentage of the intensity at the two points $\pm \frac{w}{2}$:

$$\frac{1}{C} \int_{-\infty}^{-\frac{w}{2}} e^{\frac{-2x^2}{w^2}} dx = 0.84 \tag{4}$$

$$\frac{1}{C} \int_{-\infty}^{+\frac{w}{2}} e^{\frac{-2x^2}{w^2}} dx = 0.16 \tag{5}$$

Then the width is the difference between the two positions (in mm) where the two values $0.84 P_{total}$ and $0.16 P_{total}$ are detected, as Fig. 13 shows. P_{total} is the total power of the beam before using the knife-edge.
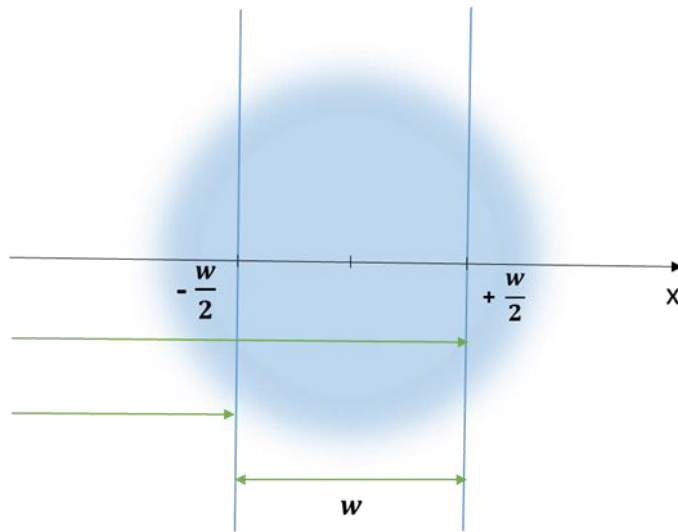
Fig. 13: The knife-edge method criterion for measuring beam width

22

This knife-edge method, based on 16% - 84% of the total power, is used to measure the beam size at three different locations along the propagation direction. First, the knife-edge is fixed on a translational stage that moves in the vertical direction, and a power meter is placed at a fixed position after the knife-edge to detect the change in the power. The knife-edge is moved by hand to cut the beam so that 84% of the total power is detected, then moved further until 16% is detected. Then the readings of the translational stage at the two locations are subtracted to get the difference between them. The absolute value of this difference gives the beam width at that particular location. Then the steps above are repeated at another two locations. Following the same procedure in the horizontal direction reveals the horizontal width of the beam. For Gaussian beams, the horizontal and vertical widths at a particular location are equal.

The next step is to find the beam waist of the laser source by solving equation (2) at two locations for two unknowns w_0 and z_1. Having the beam size at three locations with the distances between them allows for solving three pairs of equations and get three values for the beam waist and how far it is from the first location. Averaging the three values gives the experimental result of the beam waist w_0 and the distance z_1 between the waist and first location. At this point, a good picture of the Gaussian beam profile of the laser source is available and the mode-matching procedure can take place.

4.2 Mode-Matching the Frequency Comb to the Multi-Reflection Cell

Now comes the need to mode match the light beam coming from the mid-infrared frequency comb laser source to the multi-reflection optical cell. To do the mode-matching one needs two focusing lenses with different focal lengths that will provide the desirable waist size and are suitable for the available space on the optical table. It is not always trivial to find the right focal lengths that meets these requirements.

This experiment uses three lenses, one as a collimating lens to collimate the mid-infrared beam and reduce the diffraction losses, and two as mode-matching lenses. The collimating lens has a focal length $f_1 = 500$ mm, where the focal lengths of the mode-matching lenses are $f_2 = 50$ mm and $f_3 = 100$ mm consequently. The second mode-matching lens, which is $f_3 = 100$ mm, is fixed on a one-dimensional translational stage. The distance between the two mode-matching lenses can be controlled with the movement of the stage, which changes the size of the waist afterwards. The other two lenses are fixed on the optical table.

Using equation (3) with the radius of curvature of the cavity mirrors; R = 1000 mm, and the middle position where the new beam waist will be; z = 500 mm, the calculated new beam waist is $w_0 = 0.7192$ mm. The actual beam waist of the laser, which is $w_0 = 0.557$ mm, was determined experimentally in the last section with the Knife-edge method. Fig. 14 shows a schematic of the propagation of the beam with the three lenses in place; the collimating lens and the two mode-matching lenses.
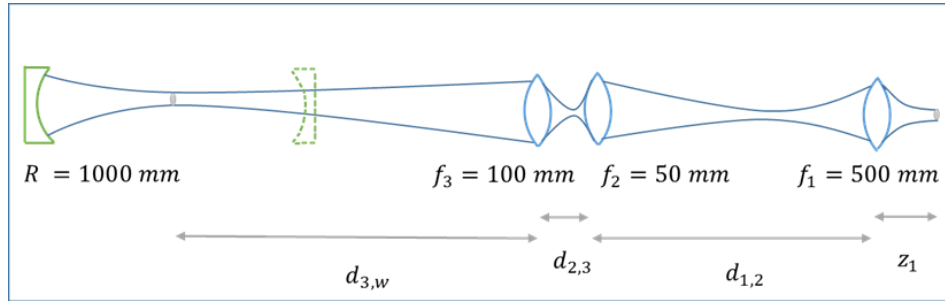
**Fig. 14 : An illustration of the mode-matching**

A computer program called BeamSim is used to obtain the required values of the distances between the waist of the laser beam and the first lens, between the first two lenses, the second and the third, and between the third lens and the middle position of the multi-reflection optical cell where the new beam waist will be located. For the program to do the calculation, the laser's beam waist obtained in section 4.1; $w_0 = 0.557$ mm, and its central wavelength; $\lambda = 3.25$ x 10^{-3} mm, are given to the program as inputs.

4.3 Alignment of the Multi-Reflection Optical Cell

At this stage, the multi-reflection optical cell has been aligned with a red alignment laser, as discussed in chapter II. Now is the time to align it with the mid-infrared laser beam. A flipping mirror and a fixed mirror, shown in Fig. 15, are used to align the mid-infrared laser beam. The flipping mirror is placed in the path of the red alignment laser so that it can be flipped at any time, when needed, to realign the multi-

reflection cell. These two mirrors are adjusted to have an overlap of the two beams, alignment and mid-infrared, so that the mid-infrared beam almost follows the same spot pattern of the red beam and thus has the same number of reflections; i.e. the same absorption path length.

After the beam reflects 579 times inside the optical cell, it exits the cell from the same aperture. After that the output beam passes through a beam splitter, and a power meter is used to detect the portion of the beam reflected form the beam splitter. The red-infrared alignment mirrors can be further adjusted until the maximum output power of the mid-infrared beam is detected.
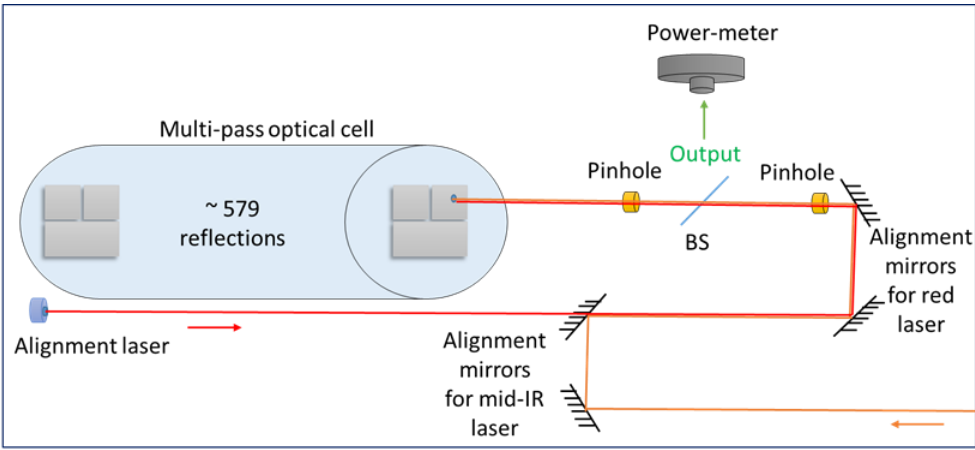

Fig. 15 : Schematic of the alignment of multi-reflection cell

## 4.4 Dual Comb Absorption Spectroscopy as an Application

So far, the mid-infrared laser beam has been mode-matched and well-aligned with the multi-reflection optical cell. The next step is to set up the elements of dual comb spectroscopy. The frequency comb with larger power and larger repetition rate is considered here as comb1, where the second as comb2, which is the opposite of the case in Fig. 1. The repetition rate difference is $\Delta f_r = 1.48$ KHz.

The mid-infrared dual comb experimental setup is illustrated in Fig. 16. The beam coming from comb2 is focused by a lens and redirected to a beam splitter. It is combined with the beam of comb1 at the beam splitter and then the two are redirected by a mirror into a photo-detector. Since the spatial overlapping, the mode-matching, and the polarization of the two beams are important factors in dual comb experiments, they are considered before placing the last mirror before the detector. After checking that the beams overlap properly, the mirror is placed and adjusted until the signal appears on the oscilloscope screen.
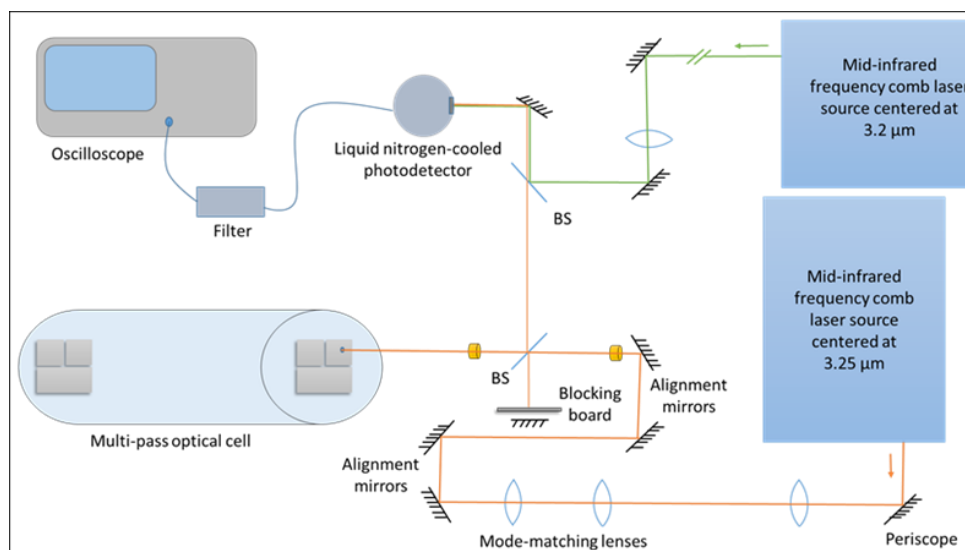
Fig. 16 : Schematic of dual comb Fourier transform experimental setup

The detector used in this setup, which can be seen in Fig. 17, is a liquid nitrogen-cooled photo-detector that allows sensitive detection of the dual comb signal. It is a HgCdTe (MCT) photo-detector with a bandwidth of 100 MHz. It is connected to a high-pass filter then to an oscilloscope of 8 bit resolution. The recorded dual comb signal is an interferogram that is later analyzed by a computer program to get the FFT and thus the absorption spectrum of the molecules present in the multi-reflection optical cell.
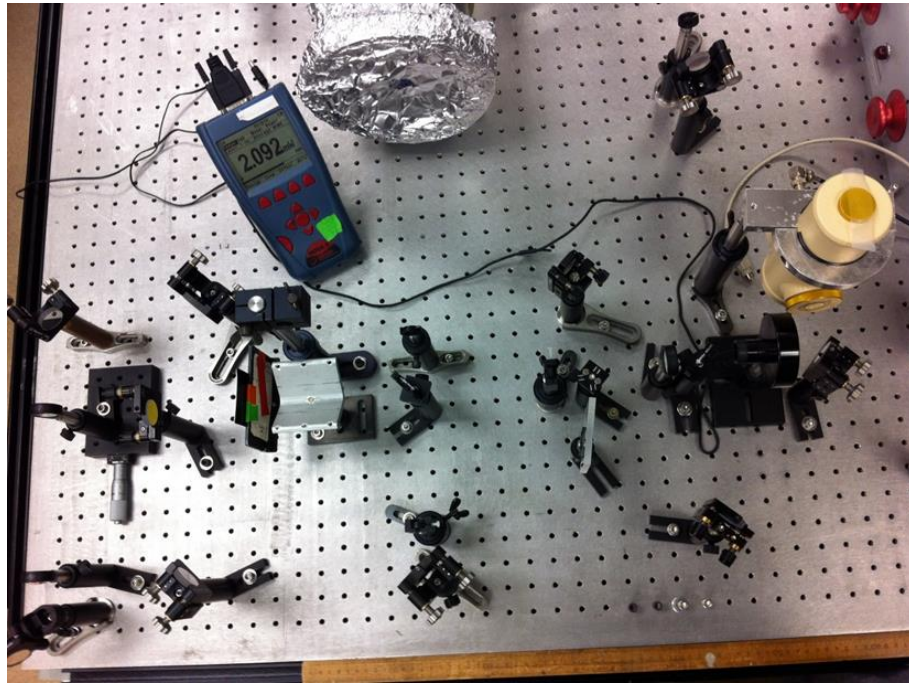
Fig. 17 : Dual comb experimental setup on the optical table

This experimental setup has been used for detection of CH_4 in ambient air inside our laboratory. This has been done in three steps. First, the output beam from the multi-reflection cell is blocked and the blocking board in Fig. 17 is removed in order to get a reference interferogram without having the beam passing through a gas sample. Second, with the blocking board removed, a small glass cell containing a mixture of CH_4 and other gases is placed in its position, and the beam out of the multi-reflection cell remains blocked. In the third step, the blocking board is back in its place and the output beam from the multi-reflection optical cell is used to get the third interferogram.
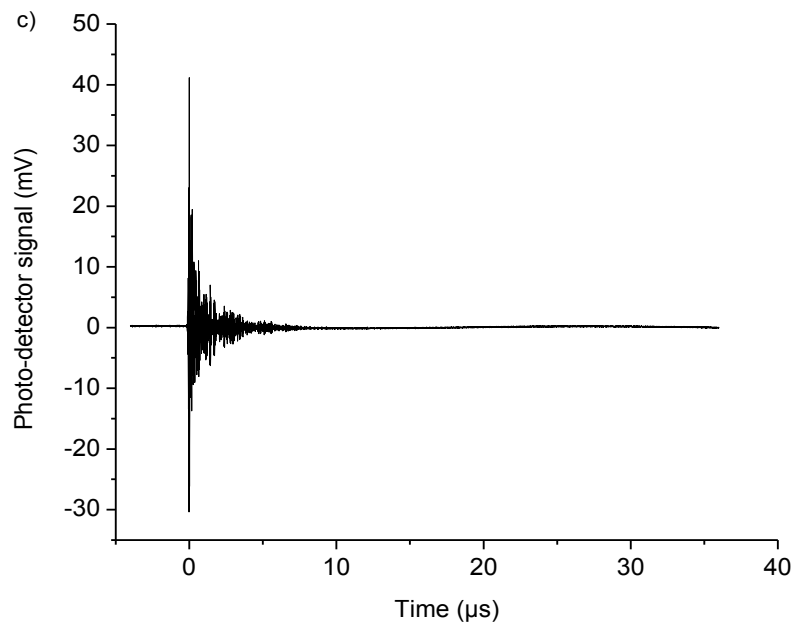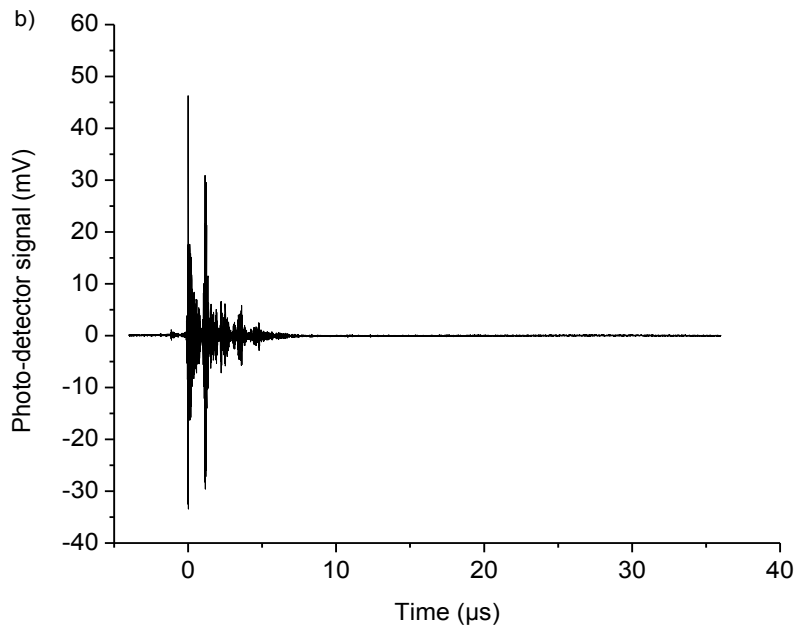
The three interferograms are shown in Fig. 18 respectively. In recording each of these interferograms, the signal is AC-coupled, the oscilloscope averages 64

interferograms with a sampling rate of 250 MS/s. The recording length is 40 µs, and the difference in the repetition rates of the two frequency combs is $\Delta f_r = 1.48$ KHz, with a total power of 1.5 mW incident from each frequency comb on the detector.

The signal appearing after the center burst in Fig. 18 (c) indicates the presence of methane molecules in the air inside the multi-reflection optical cell. This signal is stronger in Fig. 18 (b) due to the higher concentration of methane molecules in the small gas cell. The result from the second interferogram with higher concentration of methane is used for comparison between the absorption lines in the two cases, form the multi-reflection optical cell and from the small gas cell.
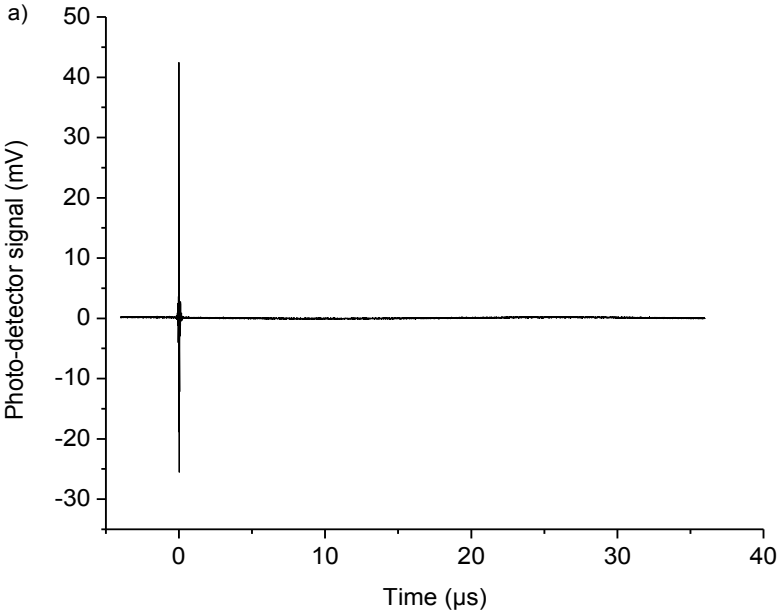

Fig. 18 : (a) A reference interferogram, (b) an interferogram with a methane gas cell present, and (c) an interferogram with the multi-reflection cell

b)

c)

Fig. 18: Continued

31

The interferograms are then transformed to the frequency domain using a MatLab program. The reference FFT signal is used for normalization of the other two FFT signals. The FFT experimental spectra in the three cases are shown in Fig. 19, which is a screen image for the FFT spectra generated by the oscilloscope.
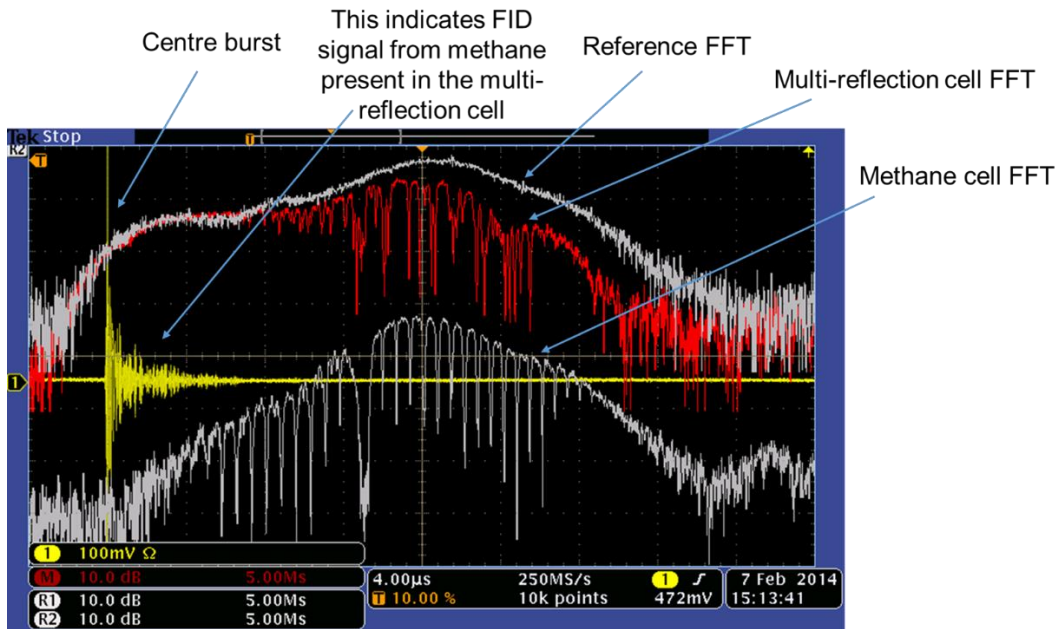
Fig. 19 : A picture of the scope's screen indicating the FFT spectra in the three cases; a reference, with methane gas cell, and with multi-reflection optical cell

Theoretical absorption spectra using HITRAN database [13] are generated to associate the experimental absorption lines with the corresponding theoretical lines for methane molecules CH_4 and water vapor molecules H_2O in the mid-infrared region.

A final result for this experiment is presented in Fig. 20. The HITRAN spectra are on the top and the dual comb experimental spectrum is on the bottom. Based on the

agreement of the experimental spectrum with HITRAN spectrum, it is concluded that the concentration of CH_4 in the laboratory's environment is about 1.2 ppmv, where for H_2O it is estimated to be around 0.12% corresponding to a relative humidity level ~ 4%. This humidity level is calculated using the vapor saturation pressure at room temperature, and an air density of 2.504×10^{19} per cubic centimeter.
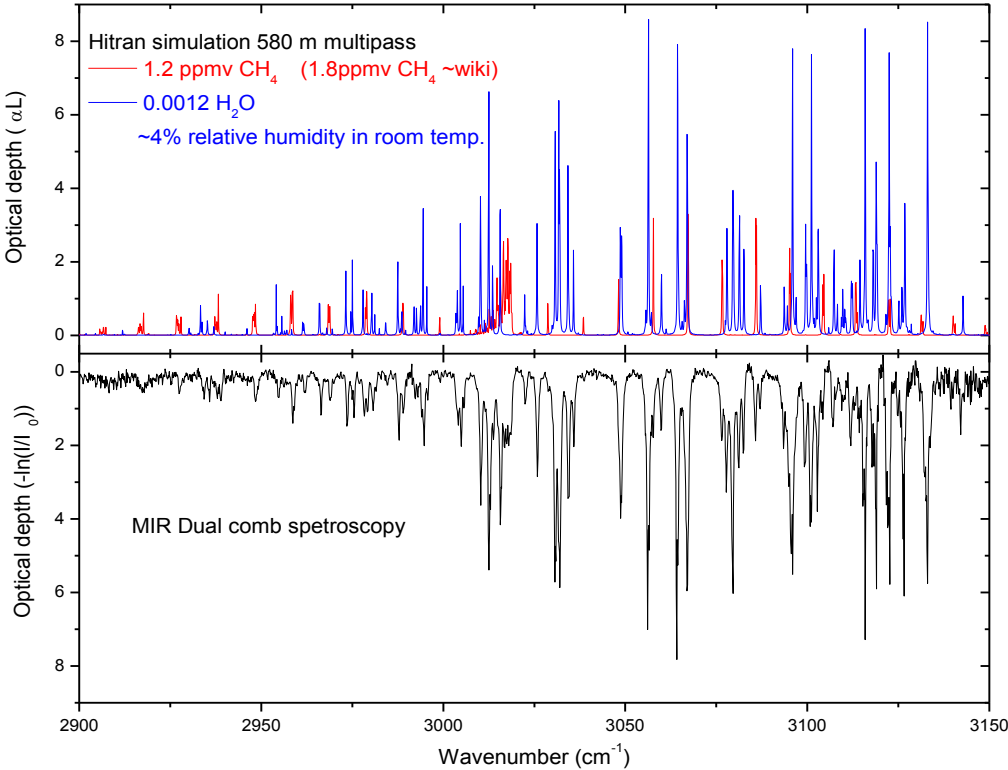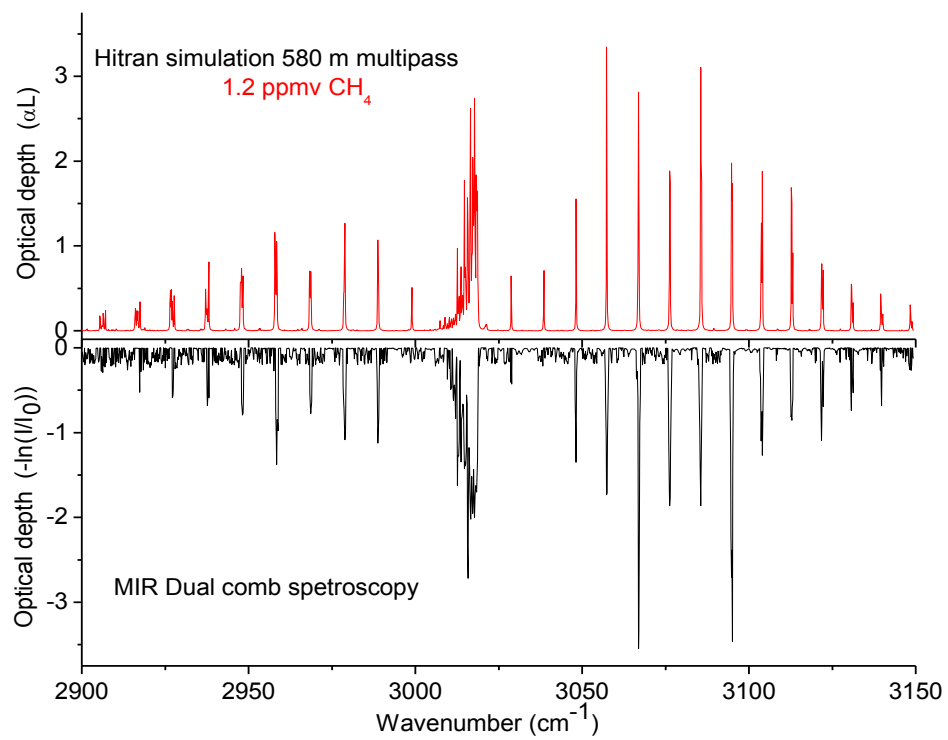

Fig. 20 : Absorption spectrum of methane in ambient air using dual comb spectroscopy in the mid-infrared

The resolution of the spectrum is 4.2 GHz, corresponding to 0.14 cm^{-1} which was obtained directly from the data. It is in a good agreement with the 4.22 GHz spectral

resolution calculated form $\dfrac{1}{Recording\ length}$ x $\dfrac{f_r}{\Delta f_r}$ with a recording length of 40 μs, a repetition rate f_r = 250 MHz, and a difference of 1.48 KHz in the repetition rates of the two combs, which are the values used in the experiment. The oscilloscope is set to average 64 interferograms, thus the time needed to get the normalized spectrum, i.e. methane absorption spectrum and the reference spectrum, is 2 x (64 x $\dfrac{1}{\Delta f_r}$) which is < 100 ms.

The signal-to-noise ratio is also estimated in this experiment since it is one of the most important elements in the analysis of spectroscopic measurements. Taking the ratio of a selected high intensity absorption line from methane's absorption spectrum, in Fig. 20, to the standard deviation of noise gives a signal-to-noise ratio (SNR) of ~ 33. Using this signal-to-noise ratio and the estimated concentration of methane from Fig. 20, this experiment provides a 3σ minimum detection limit (MDC) of 100 ppbv for methane in the ambient air.

In a further step, a filtered absorption spectra, shown in Fig. 21, is generated for methane in ambient air from the results of Fig. 20 with the same spectral resolution. The water vapor lines are filtered out using a program with a threshold level. The data under the threshold level are kept the same and those above threshold are analyzed in two steps by comparing them to the theoretical lines. First, the water lines are eliminated in regions where no methane lines are present. Then, the lines in the regions where overlapping happen are multiplied by a ratio extracted from the theoretical data. Fig. 21 shows a good agreement between the experimental dual comb absorption spectrum and HITRAN [13] spectrum for 1.2 ppmv of methane in the air.

Fig. 21 : Comparison between Hitran and filtered dual comb spectra for methane in ambient air

CHAPTER V

CONCLUSIONS AND FUTURE WORK

5.1 Sensitivity and Selectivity of the Absorption Measurements

The sensitivity is one of the most important factors in high precision molecular spectroscopy. It can be improved with a more efficient mode-matching of the laser source to the multi-reflection optical cell, and a better alignment of the optical cell. It is also crucial to consider the noise sources in the surrounding environment which highly contributes to the signal-to-noise ratio and thus to the sensitivity of the absorption measurements. From the experimental absorption lines of methane in ambient air in Fig. 20, the signal-to-noise ratio (SNR) is estimated in this experiment to be around 33.

The selectivity is another main factor in molecular spectroscopy. It can be addressed by means of a broadband laser source that allows for a detection of several trace gas molecules. The mid-infrared frequency comb laser sources used in this experiment emit light of frequencies that range over a broadband which promises a wide variety of spectroscopic applications for various trace gas molecules.

Temperature and humidity in the laboratory's environment also play an essential rule in both the sensitivity and the selectivity of the absorption measurements. As the temperature effects the broadening of the line shapes, the humidity results in more water vapor absorption and thus a lower output power from the multi-reflection cell. And because of such effects, it is preferred to take the experimental data when the outside

temperature is stable and the humidity level is low. The absorption spectra revealed in this experiment is taken in a day of a relatively low humidity level ~ 4%.

The spectral resolution of the absorption spectra obtained in this experiment with dual frequency comb spectroscopy for methane in ambient air; a 4.2 GHz resolution, is one order of magnitude better than that with the use of a monochromator; a 60 GHz resolution. In addition, getting the final absorption spectrum with dual comb spectroscopy requires at most an acquisition time of 100 ms, where the slow scanning speed of the monochromator requires a time interval of 20 min for a single spectrum. This emphasizes on the importance of dual comb spectroscopy as a short-time precise spectroscopic technique.

5.2 Future Improvements

The experimental result presented in Fig. 20, for methane in the multi-reflection cell, shows weaker absorption lines than those in Fig. 19 for the small gas cell. This helps to understand how a higher concentration of CH_4 molecules in a gas sample leads to higher precision for the spectral lines, in an agreement of equation (1), which in turn suggests another approach for this experiment. This approach will be done by evacuating the cell and filling it with calibrated gas mixtures. With evacuation and using dry gases, the water vapor in the air will not contribute to the absorption signal, and thus more accurate detection limit will be achieved. Moreover, this approach will allow for more complete characterization of the multi-reflection cell implemented in this experiment.

Sensitivity and spectral resolution of the absorption measurements can also be enhanced

by increasing the recording length and by using a larger repetition rate difference.

REFERENCES

[1] X. Cui, C. Lengignon, T. Wu, W. Zhao, G. Wysocki, E. Fertein, C. Coeur, A. Cassez, L. Croize, W. Chen, Y. Wang, W. Zhang, X. Gao, W. Liu, Y.Zhang, F. Dong, J. Quan. Spec. & Rad. Trans. 113, 1300-1316 (2012).

[2] F. K Tittle, D. Richter. A. Fried, ed. by I. T. Sorokina, K. L. Vodopyanov (Top. Appl. Phys. 89) (Springer, Berlin Heidelberg New York, 2003), 445-510.

[3] H. Dahnke, D. Kleine, W. Urban, P. Hering, M. Mürtz, Appl. Phys. B 72, 121-125 (2001).

[4] M. J. Thorpe, J. Ye, Appl. Phys. B 91, 397-414 (2008).

[5] F. Zhu, T. Mohamed, J. Strohaber, A. A. Kolomenski, Th. Udem, H. A Schuessler, Appl. Phys. Lett. 102, 121116 (2013).

[6] A. Foltynowicz, P. Masłowski, A. J. Fliesher, B. J. Bjork, Jun Ye, Appl. Phys. B 110, 163-175 (2013).

[7] C. Robert, Appl. Opt. 46, 5408-5418 (2007).

[8] B. H. Lee, E. C. Wood, M. S. Zahniser, J. B. McManus, D. D. Nelson, S. C. Herndon, et al, Appl. Phys. B 371, 417 -23 (2011).

[9] A. Schliesser, N. Picqué, T. W. Hänsch, Nature Photonics 6, 440-449 (2012).

[10] W. Demtröder, *Laser Spectroscopy* (Springer, New York, 2008).

[11] S. T. Cundiff and J. Ye, *Femtosecond Optical Frequency Comb Technology* (Springer, New York, 2005).

[12] J. T. Verdeyen, *Laser Electronics* (New Jersey: Prentice-Hall, Inc., Englewood Cliffs, 1981).

[13] L. S. Rothman, I. E. Gordon, A. Barbe, D. C. Benner, P. F. Bernath, M. Birk, V. Boudon, L. R. Brown, A. Campargue, J. P. Champion, K. Chance, L. H. Coudert, V. Dana, V. M. Devi, S. Fally, J. M. Floud, R. R. Gamache, A. Goldman, D. Jacquemart, I. Kleiner, N. Lacome, W. J. Lafferty, J. Y. Mandin, S. T. Massie, S. N. Mikhailenko, C. E. Miller, N. Moazzen-Ahmadi, O. V. Naumenko, A. V. Nikitin, J. Orphal, V. I. Perevalov, A. Perrin, A. Predoi-Cross, C. P. Rinsland, M. Rotger, M. Simeckova, M. A. H. Smith, K. Sung, S. A. Tashkun, J. Tennyson, R. A. Toth, A. C. Vandaele, J. V. Auwera, *The HITRAN 2008 Molecular Spectroscopic Database*, J. Quant. Spectrosc. Radiat. Transfer 110, 553-572 (2009).

APPENDIX A

ANALYSIS OF MINIMUM REFLECTIVITY

The mid-infrared reflectivity of the mirrors which are used in the multi-reflection optical cell is considered in this section. The power of the mid-infrared frequency comb used here is 60% of the total power, i.e. $P > 200$mW. As the beam arrives at the beam splitter, its power is around 100 mW. The beam splitter, as suggested by the manufacturer, has a 55% transmittance and a 45% reflectivity. However, it is indicated in this experiment that it has a 70% transmittance and a 30% reflectivity, as shown in Fig. 22. Thus, an input power of 70 mW is incident into the multipass cell, and the detected power after reflection from the beam splitter is 1.6 mW, referring to 5 mW output power from the multipass cell.
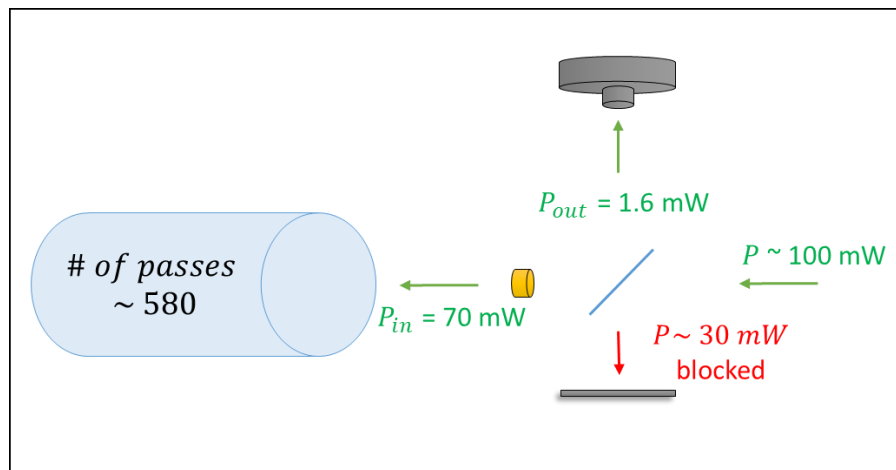
Fig. 22: Power detection scheme towards revealing the minimum reflectivity

Then the following relation (6) is used:

$$\frac{P_{out}}{P_{in}} \sim (A \ x \ R \ x \ D)^N \qquad\qquad (6)$$

where A refers to absorbance, R to reflectivity, D for diffraction losses, and N to the number of reflections inside the optical cavity. Assuming A=1 and D=1, and substituting with the number of reflections N = 579 in (7), it follows:

$$\frac{5 \ mW}{70 \ mW} \sim (R)^{579} \qquad \rightarrow \qquad R = \sqrt[579]{\frac{5 \ mW}{70 \ mW}} = 0.9955 \qquad\qquad (7)$$

In conclusion, the reflectivity of the mirrors in the mid-infrared is R ≥ 99.55% comparing to R = 99.9% as the manufacturer who provided the mirrors suggests.